PARTICULATE SCIENCE AND TECHNOLOGY
2018, VOL. 36, NO. 2, 194–201
http://dx.doi.org/10.1080/02726351.2016.1240127

Taylor & Francis
Taylor & Francis Group

Kinetics behavior of methylene blue onto agricultural waste

Çiğdem Sarici-Özdemir[a] and Fatih Kiliç[b]

[a]Department of Chemical Engineering, Faculty of Engineering, Inonu University, Malatya, Turkey; [b]Department of Chemical Engineering, Faculty of Engineering, Tunceli University, Tunceli, Turkey

ABSTRACT

In the present work, investigations on a potential use of agricultural waste for the removal of methylene blue (MB) from wastewater are presented. Adsorption kinetics of MB has been studied using reaction-based and diffusion-based models. Three kinetic models, namely pseudo-first-order, pseudo-second-order, and the Elovich are analyzed at the temperature of 298 K for the reaction-based model. The kinetic studies showed that the data were well described by the pseudo-second-order kinetic model. Intraparticle diffusion, external-film diffusion, and internal-pore diffusion models characterizing MB were obtained. The results suggested that the agricultural waste has a high potential to be used as an effective adsorbent for MB adsorption. Pseudo-first-order, pseudo-second-order, and the Elovich models were employed to describe the desorption mechanism. The experimental results showed that the pseudo-second-order equation is the best model.

KEYWORDS

Adsorption; agricultural waste; almond shell; kinetic studies; methylene blue

1. Introduction

This article brings together the environmental problems in developing technology. Among these problems, population growth, and urbanization, ineluctable place greater demands on the world. With industrial revolution synthetic dyes are being in universal use by different industries. With advantages as cheaper to produce, more brighter colors, fast and easy to apply to fabric, the new dyes changed world. The dying process includes aniline, dioxin, toxic heavy metals which are harmful chemicals (such as chrome, copper, zinc, formaldehyde). Approximately all industrial dye processes involve a solution of a dye in water in which the fabrics are soaked. Therefore the textile factories across the world are dumping dye effluent into rivers. Accordingly, it is necessary to remove them from the wastewater before discharging. Physical, chemical, and biological methods have been investigated to remove these materials. Among the methods, removal of dyes by adsorption is counted as one of the competitive methods because of high efficiency, economic feasibility, and simplicity of design/operation (Chen et al. 2010; Rafatullah et al. 2010; Haque, Jun, and Jhung 2011).

Agricultural wastes, because of their large surface area and relatively high sorption capacity, for a wide variety of dyes, have become the most promising and effective adsorbent. Nevertheless, their applications are restricted, because agricultural wastes are prepared from natural materials (such as rice husks, coconut husks, sawdust, *Tamrix articulata*) (Othman et al. 2012, 2013). Textile waste containing cotton, nylon, and polymers creates a problem in the world. Agricultural waste prepared from wastes could be important for the regional economy. Because high-value products are obtained from low-cost materials, they simultaneously bring solution to the problem of wastes (Altenor et al. 2009). Methylene blue (MB) is one of the well-known basic/cationic dyes and has been widely used in wood, silk, cotton, pharmaceutical industries.

In this work, agricultural waste has been prepared from almond shell (AS). The prepared agricultural waste is used as an adsorbent to remove MB from aqueous solutions. The kinetics and diffusion parameters of the adsorption processes have been investigated. The particle sizes were less than 125 μm. The x-ray diffractogram and SEM of AS are given in Figure 1. When the figure of XRD is scrutinized, it is seen that the AS sample includes amorphous structure. According to SEM photograph of the AS, it has got microporosity.

2. Material and methods

2.1. Materials

The solute selected for this work was MB (chemical formula = $C_{16}H_{18}N_3SCl$, MW = 320 g/mol). A stock solution of 100 ppm was prepared by dissolving the required amount of MB in distilled water. The spectrophotometric determination of MB was carried out using a Shimadzu UV/Vis spectrophotometer at 662 nm (model UV-2100S, Japan).

2.2. Preparation of agricultural waste (almond shell)

Adsorbent used in this study was AS. AS sorbent was transferred to an oven set at 50°C for 24 h to reduce the water content. The dried sorbent was crushed and milled. The particle sizes were less than 125 μm.

2.3. Adsorption experiments

MB solutions were prepared in distilled water at the desired temperature. Adsorption experiments were carried out by agitating 0.1 g of AS with 50 cm^3 solutions at different values of

CONTACT Çiğdem Sarici-Özdemir cigdem.ozdemir@inonu.edu.tr Department of Chemical Engineering, Faculty of Engineering, Inonu University, Malatya, Turkey.

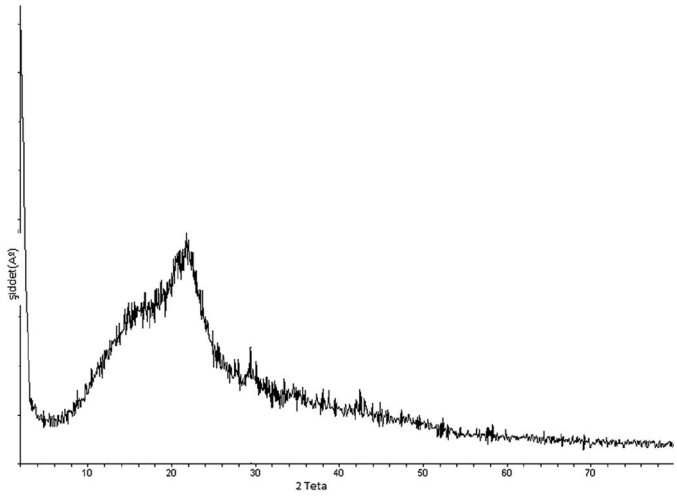

(a)

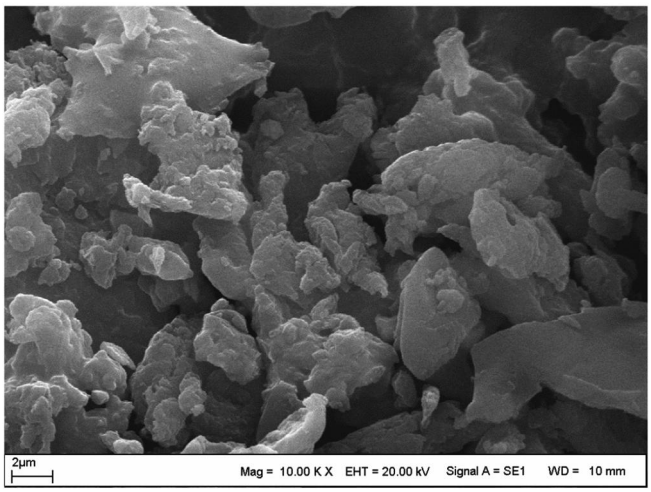

(b)

Figure 1. (a) X-ray diffractogram of PS, (b) scanning electron micrographs of AS.

time (1–120 min) and 25°C in a thermostatic bath operating at 400 rpm. The amount of MB adsorbed onto AS, q_t (mg/g), was calculated by the mass balance relationship represented by equation:

$$q_t = \frac{(C_0 - C_t)}{V/W}, \quad (1)$$

where C_0 and C_t are the initial and final (at time t) liquid and phase concentrations of MB (mg/L), respectively, V is the volume of the solution (L), and W is the weight of the dry AS used (g).

2.4. Error functions

In past years, linear regression has been one of the most practicable tool describing the best-fitting relationship quantifying the distribution of adsorbates, mathematically analyzing the adsorption systems. Nonlinear optimization ensures method for defining isotherm parameter values but still demands an error function assessment, to evaluate the fit of the isotherm to the experimental results. Whereby the choice of error function could affect the parameters reproduced. In this study, eight nonlinear error functions (sum squares errors, hybrid fractional error function, Marquardt's percent standard deviation, average relative error, sum of absolute error, the coefficient of determination, nonlinear χ^2 test, and standard deviation of relative errors) (Table 1) were investigated. Contrary to the linearization models, nonlinear regression usually requires the minimization or maximization of error distribution (between the experimental data and the predicted isotherm) based upon its convergency criteria (Kumar, Porkodi, and Rocha 2008).

Table 1. List of error functions.

Error function	Abbreviation	Definition
Sum squares errors	ERRSQ	$\sum_{i=1}^{p} \left(q_{exp} - q_{cal}\right)_i^2$
Hybrid fractional error function	HYBRID	$\frac{100}{p-n} \sum_{i=1}^{p} \left[\frac{\left(q_{exp}-q_{cal}\right)^2}{q_{exp}}\right]_i$
Marquardt's percent standard deviation	MPSD	$100\left[\sqrt{\frac{1}{p-n}\sum_{i=1}^{p}\left(\frac{q_{exp}-q_{cal}}{q_{exp}}\right)^2}\right]_i$
Average relative error	ARE	$\frac{100}{p} \sum_{i=1}^{p} \left(\frac{\lvert q_{exp}-q_{cal}\rvert}{q_{exp}}\right)_i$
Sum of absolute error	EABS	$\sum_{i=1}^{p} \lvert q_{exp} - q_{cal}\rvert_i$
The coefficient of determination	R^2	$\frac{\left(q_{exp}-\overline{q_{cal}}\right)^2}{\sum \left(q_{exp}-\overline{q_{cal}}\right)^2+\left(q_{exp}-q_{cal}\right)^2}$
Nonlinear χ^2 test	χ^2	$\sum_{i=1}^{p} \frac{\left(q_{exp}-q_{cal}\right)^2}{q_{exp}}$
Standard deviation of relative errors	SRE	$\sqrt{\frac{\sum_{i=1}^{p}\left[\left(q_{exp}-q_{cal}\right)_i - \mathrm{ARE}\right]_i^2}{p-1}}$

3. Results and discussion

3.1. Effect of temperature on the adsorption of MB

The effect of temperature on the removal of MB onto AS is presented in Figure 2. It was seen that as the adsorption temperature was increased from 298 to 323 K for the adsorption capacities of MB decreased with the temperature at the end of 120 min. The fact that the rate of adsorption decreases with an increase in temperature indicates that the mobility of the MB molecules decreases with an increase in the temperatures.

3.2. Adsorption isotherm and kinetic models

The application of adsorption isotherms is a precondition to understand the adsorbate–adsorbent interaction. There are many equations to analyze experimental adsorption equilibrium data. Langmuir and Freundlich equations are the most accepted surface adsorption models for single-solute systems. Nevertheless, an interesting trend in the isotherm modeling is the derivatization in more than one approach, in this way directing to the difference in the physical interpretation of the model parameters (Ruthven 1984). In this study, the isotherm of two parameters Langmuir (1918), Freundlich (1906) Dubinin–Radushkevich (Dubinin and Radushkevich 1947), Temkin (Temkin and Pyzhev 1940), and Frumkin (Sarıcı-Ozdemir 2014) and three parameters Redlich–Peterson (RP; Redlich and Peterson 1959), Sips (1948), Toth (1971), Radke–Prausnitz (Kumar, Porkodi, and Rocha 2008), and Koble–Corrigan (Koble and Corrigan 1952) were studied. Table 2 shows the equations and constants of such isotherms. Figures 3 and 4 show graphs obtained by using the equation.

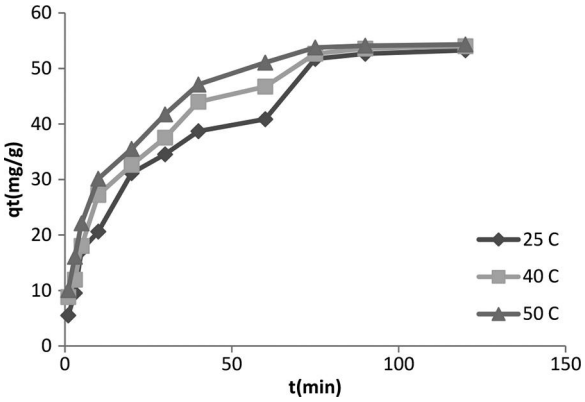

Figure 2. Effect of temperature on the adsorption of MB as a function of time at 200 ppm.

All the parameters of the isotherm model for the adsorption of MB onto AS are illustrated in Tables 3–5 at different temperatures. It can be seen from tables that when the values of R^2 were compared, the adsorption of MB onto AS showed an inclination to follow the Langmuir isotherm for two parameters and RP for three parameters. Error analysis also shows the minimum value for all temperatures in the Langmuir isotherm and RP.

3.2.1. Reaction-based models

To investigate the adsorption kinetics of MB, three kinetic models, namely pseudo-first-order, pseudo-second-order, and Elovich models, were analyzed at the concentration of 200 ppm.

The rate constant for the adsorption of MB onto AS determined by the pseudo-first-order equation is expressed as (Barrett et al. 1951):

$$\frac{dq}{dt} = k_1(q_e - q), \tag{2}$$

where k_1 (min^{-1}) is the pseudo-first-order rate constant. Integrating Equation (3) with respect to the integration conditions $q = 0$ to $q = q_t$ at $t = 0$ to $t = t$, the kinetic rate expression becomes:

$$\log(q_e - q_t) = \log q_e - \frac{k_1}{2.303}t, \tag{3}$$

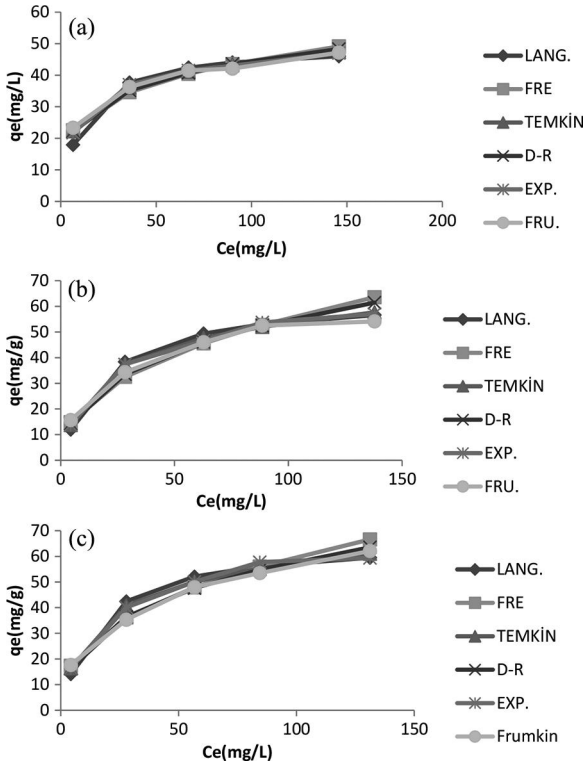

Figure 3. Two parameters ısotherms of methylene blue at: (a) 25°C, (b) 40°C, and (c) 50°C.

where q_e and q_t are the amounts of MB adsorbed (mg/g) at equilibrium and time t (min), respectively.

The adsorption kinetics have also been determined by the pseudo-second-order model using equation (Ho and McKay 1998):

$$\frac{1}{(q_e - q_t)} = \frac{1}{q_e} + k_2 t. \tag{4}$$

where k_2 is the second-order-rate constant (g/mg · min) and $h = k_2 q_e^2$, where h is the initial adsorption rate (mg/g · min).

The Elovich equation is expressed as follows:

$$\frac{dq}{dt} = \alpha e^{(\beta q_t),} \tag{5}$$

where α is the initial adsorption rate (mg/g · min) and β is the

Table 2. List of isotherm equilibrium.

Isotherm	Nonlinear form	Linear form	Plot
		Two parameters	
Langmuir	$q_e = \frac{Q_o b C_e}{1+bC_o}$	$\frac{C_e}{q_e} = \frac{1}{bQ_o} + \frac{C_e}{Q_o}$	$\frac{C_e}{q_e}$ vs. C_e
Freundlich	$q_e = K_F C_e^{1/n}$	$\ln q_e = \ln K_f + \frac{1}{n}\ln C_e$	$\ln C_e$ vs. $\ln q_e$
Dubinin–Radushkevich	$q_e = (q_m)\exp(-k_{ad}\varepsilon^2)$	$\ln q_e = \ln q_m - k_{ad}\varepsilon^2$	$\ln q_e$ vs.ε^2
Temkin	$q_e = \frac{RT}{b_T}\ln A_T C_e$	$q_e = \frac{RT}{b_T}\ln A_T + \left(\frac{RT}{b_T}\right)\ln C_e$	Q_e vs. $\ln C_e$
Frumkin	$\frac{\theta}{(1-\theta)}e^{-2a\theta} = k.C_e$	$\ln\left[\left(\frac{\theta}{1-\theta}\right).\frac{1}{C_e}\right] = \ln k + 2a\theta$	$\ln\left[\left(\frac{\theta}{1-\theta}\right).\frac{1}{C_e}\right]$ vs. θ
		Three parameters	
Redlich–Peterson	$q_e = \frac{K_R C_e}{1+a_R C_e^{\beta}}$	$\ln\left(K_R\frac{C_e}{q_e} - 1\right) = \beta\ln(C_e) + \ln(a_R)$	$\ln\left(K_R\frac{C_e}{q_e} - 1\right)$ vs. $\ln C_e$
Sips	$q_e = \frac{K_s a_s C_e^s}{1+a_s C_e^s}$	$s\ln(C_e) = -\ln\left(\frac{K_s}{q_e}\right) + \ln a_s$	$\ln\left(\frac{K_s}{q_e}\right)$ vs. $\ln C_e$
Toth	$q_e = \frac{K_T C_e}{(a_T + C_e^t)^{1/t}}$	$\ln\left(\frac{q_e}{K_T}\right) = \ln(C_e) - \frac{1}{t}\ln(a_T + C_e)$	$\ln\left(\frac{q_e}{K_T}\right)$ vs. $\ln C_e$
Radke–Prausnitz	$q_e = \frac{K_{RP}K_{RP}C_e}{\left(1+K_{RP}C_e^{\beta}\right)}$	$\frac{C_e}{q_e} = \frac{1}{K_{RP}K_{RP}} + \frac{1}{K_{RP}}C_e^{\beta}$	$\frac{C_e}{q_e}$ vs. C_e^{β}
Koble–Corrigan	$q_e = \frac{AC_e^n}{1+BC_e^n}$	$\frac{1}{q_e} = \frac{B}{A} + \frac{1}{A}\frac{1}{C_e^n}$	$\frac{1}{q_e}$ vs. $\frac{1}{C_e^n}$

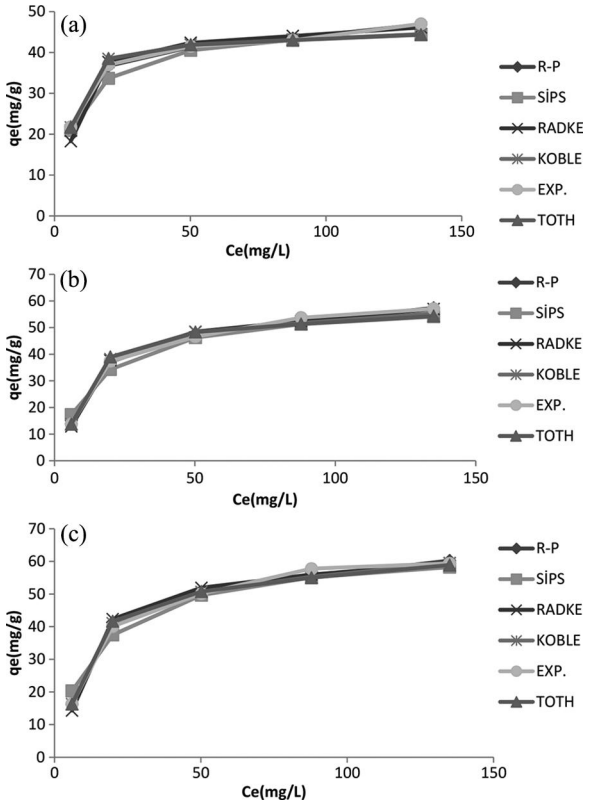

Figure 4. Three parameters ısotherms of methylene blue at: (a) 25°C, (b) 40°C, and (c) 50°C.

desorption constant (g/mg). $q_t = 0$ at $t = 0$, and $q_t = q_t$ at $t = t_t$, at which point Equation (5) becomes:

$$q_t = \frac{1}{\beta t}\ln(\alpha\beta) + \frac{1}{\beta}\ln t. \tag{6}$$

In order to understand the adsorption kinetics of MB onto AS, three kinetic models—first-order, pseudo-second-order, and Elovich—were applied to evaluate the experimental data in Figure 5.

The kinetic parameters for the adsorption are given in Table 6. The coefficient of correlation for the pseudo-first-order kinetic model was not found to be high for all temperatures. In addition, the determined values of q_e calculated from the equation differed from the experimental values, which showed that the adsorption of MB onto AS is not the first-order reaction. It can be seen from Table 6 that the determined values of q_e calculated from the equation agree with the experimental values, thus revealing that the MB adsorption onto AS follow the pseudo-second-order kinetics.

3.2.2. Diffusion-based models

Various diffusion models can be used to describe adsorption. These diffusion models have been developed to predict the dynamic character of adsorption. This work used the intra-particle diffusion, external-film diffusion, and internal-pore diffusion models to characterize adsorption of MB.

Table 3. Isotherm constant with error analysis of methylene blue at 25°C.

		Error							
Isotherm	Constants	R^2	ERRSQ	Hybrid	MPSD	ARE	EABS	X^2	S_{RE}
Langmuir		0.99	18.026	25.14838	10.479	5.215	7.409	0.755	5.713
Q_0	47,751								
B	0.088								
Freundlich		0.98	12.215	10.338	5.231	3.651	6.874	0.310	4.444
K_f	14.114								
N	3.994								
Dubinin–Radushkevich		0.99	6.024	5.114	3.829	2.527	4.824	0.153	3.022
$q_m \times 10^4$	3.358								
k_{ad}	0.0022								
Temkin		0.99	1.576	1.464	3.813	1.478	2.624	0.043	1.767
A	2.412								
B	306.512								
Frumkin		0.98	3.891	4.977	3.736	2.366	3.439	0.149	2.846
ln$k$	9.399								
A	−31.865								
Redlich–Peterson		0.99	0.357	0.290	0.846	0.001	1.103	0.008	0.298
K_R	9.780								
a_R	0.366								
B	0.88								
Sips		0.99	19.037	16.320	6.597	4.188	7.788	0.489	3.295
K_S	47.393								
a_S	0.143								
S	0.95								
Toth		0.99	9.503	7.204	4.073	2.232	4.667	0.216	1.874
K_T	46.75								
a_T	7.004								
T	0.98								
Radke–Prausnitz		0.99	15.213	20.997	4.178	4.846	6.954	0.629	6.112
K_{RP}	47.169								
k_{RP}	0.096								
P	0.99								
Koble–Corrigan		0.99	8.480	6.446	3.836	2.180	4.560	0.193	2.725
A	6.690								
B	0.141								
n	0.96								

Table 4. Isotherm constant with error analysis of methylene blue at 40°C.

		Error							
Isotherm	Constants	R^2	ERRSQ	Hybrid	MPSD	ARE	EABS	X^2	S_{RE}
Langmuir		0.99	12.532	14.627	8.492	4.751	6.708	0.439	5.749
Q_0	64.516								
B	0.052								
Freundlich		0.97	69.223	49.795	10.997	7.176	14.418	1.493	9.169
K_f	7.927								
N	2.366								
Dubinin–Radushkevich		0.99	36.053	26.135	4.789	4.968	10.427	0.784	6.182
$q_m \times 10^4$	7.351								
k_{ad}	0.0033								
Temkin		0.99	4.316	2.773	4.870	1.412	3.476	0.083	1.888
A	0.688								
B	204.084								
Frumkin		0.97	23.327	23.074	4.506	6.102	9.697	0.692	5.853
ln$k$	7.946								
a	−15.325								
Redlich–Peterson		0.99	4.220	2.762	2.346	0.003	3.434	0.082	1.027
K_R	4.820								
a_R	0.145								
B	0.87								
Sips		0.99	36.652	47.102	15.936	8.836	12.356	1.413	9.119
K_S	60.241								
a_S	0.068								
S	0.99								
Toth		0.99	18.575	12.210	4.967	3.478	8.445	0.366	2.757
K_T	61.109								
a_T	12.746								
T	0.95								
Radke–Prausnitz		0.99	5.963	5.437	5.094	2.755	4.437	0.163	3.323
K_{RP}	45.045								
k_{RP}	0.088								
P	0.93								
Koble–Corrigan		0.99	10.221	6.654	4.859	2.496	6.149	0.199	2.952
A	4.618								
B	0.071								
N	0.90								

The intraparticle diffusion equation (Weber et al. 1973; Srivastova, Tyagı, and Pant 1989) can be written as follows: where c is the intercept of the line, which is proportional to the thickness of the boundary layer and k_{int} is the intraparticle diffusion rate constant (mg/(g.min$^{-1/2}$)). The intraparticle diffusion model rate constant, k_{int}, is obtained from the slope of the straight line of q_t versus $t^{1/2}$(Figure 6).

$$q_t = k_{int} t^{1/2} + c \tag{7}$$

During the initial adsorption period, description can be simplified by assuming that the concentration at the activated carbon surface tends toward zero (intraparticle diffusion negligible). External diffusion resistance is predominant and controls the adsorption of MB. Thus, the external diffusion models can be considered as follows (Dutta et al. 2011):

$$\left[d\left(\frac{C_t}{C_0}\right) \Big/ dt\right] = -\frac{A}{V}, \tag{8}$$

and in the integrated form:

$$\ln\frac{C_t}{C_0} = k_f \times \frac{A}{V} \times t, \tag{9}$$

where C_0 is the initial MB concentration (mg/dm^3), C_t is MB concentration at time t (min), k_f is external surface diffusion coefficient (m/min), A is external surface area of the agricultural waste (125 m^2/g), V is volume of solution (dm^3). Parameter k_f can be estimated from the slope of the ln(C_t/C_0) versus t curve at time $t \to 0$.

The internal-pore diffusion can be calculated by using equations which are derived from Fick's law (Streat et al. 1995; Hajjaji et al. 2001):

$$F(t) = \frac{C_0 - C_t}{C_0 - C_e} = \frac{q_t}{q_e} = \sqrt{\left[1 - \exp\left(-\frac{\pi^2 D t}{r^2}\right)\right]} \tag{10}$$

or

$$\ln\left(1 - F(t)^2\right) = \frac{\pi^2 D}{r^2} t, \tag{11}$$

where C_e is the MB equilibrium concentration (mg/dm^3), D is the internal-pore diffusion coefficient (m^2/min), and r is the particle radius assuming spherical geometry (2×10^{-6} m). A plot of ln[1 – $F(t)^2$] versus time t should be linear with a slope of ($-\pi^2 \times D$)/r^2, which is commonly known as the diffusional rate constant.

Table 7 shows that the intraparticle diffusion model rate constant, k_{int}, which decreases as the temperature increases. This could be attributed to the driving force of diffusion. The driving force changes with temperatures in the solution. The linear plots at various concentration do not pass through the origin, which shows that the intraparticle diffusion is not the only rate-controlling step (Figure 6). If the plot is straight line passing through the origin, then the adsorption rate is governed by particle diffusion mechanism. Otherwise, it is

Table 5. Isotherm constant with error analysis of methylene blue at 50°C.

		Error							
Isotherm	Constants	R^2	ERRSQ	Hybrid	MPSD	ARE	EABS	X^2	S_{RE}
Langmuir		0.99	17.188	18.794	8.955	5.277	8.315	0.564	6.377
Q_0	66.667								
B	0.063								
Freundlich		0.97	75.856	48.645	10.113	7.069	16.011	1.459	9.117
K_f	9.821								
n	2.548								
Dubinin–Radushkevich		0.98	45.513	29.927	4.299	5.330	13.322	0.897	5.792
$q_m \times 10^4$	7.088								
k_{ad}	0.0029								
Temkin		0.99	9.453	5.545	4.218	1.826	4.939	0.166	2.556
A	0.815								
B	205.417								
Frumkin		0.97	54.680	40.135	4.100	7.236	15.213	1.204	7.314
ln$k$	7.981								
a	−20.791								
Redlich–Peterson		0.99	8.478	5.318	3.211	0.005	5.166	0.159	1.455
K_R	5.970								
a_R	0.156								
β	0.89								
Sips		0.99	31.149	42.858	14.835	7.641	10.808	1.285	8.362
K_S	66.225								
a_S	0.088								
S	0.90								
Toth		0.99	10.913	6.978	3.712	2.250	5.566	0.209	1.982
K_T	71.428								
a_T	6.034								
T	0.75								
Radke–Prausnitz		0.99	15.686	16.663	4.619	4.979	7.971	0.499	5.839
K_{RP}	63.291								
k_{RP}	0.068								
P	0.99								
Koble–Corrigan		0.99	7.575	4.648	4.221	1.700	4.285	0.139	2.198
A	6.575								
B	0.090								
n	0.80								

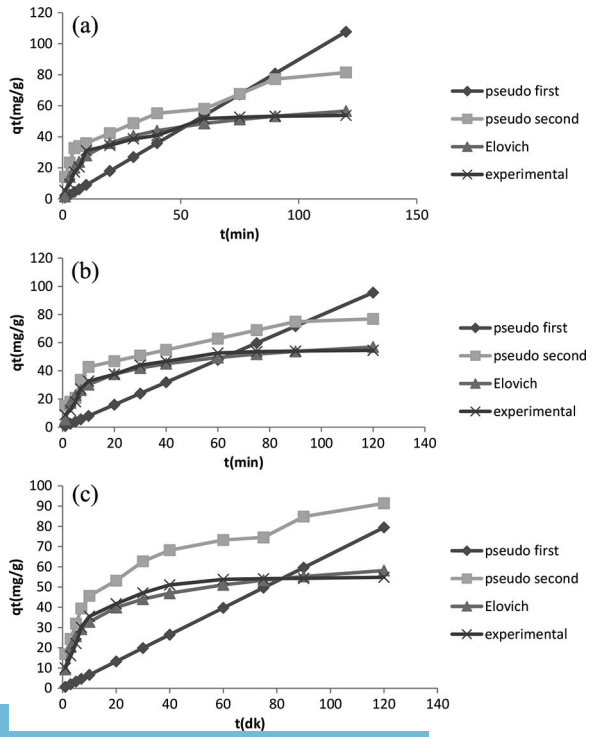

Figure 5. Comparison of kinetic models at 200 ppm concentration of MB solutions: (a) at 298 K, (b) at 313 K, (c) at 323 K.

governed by the film diffusion. The values of c are related to the boundary layer resistance. It is relatively high, and the greater is the contribution of the surface adsorption in the rate-limiting step.

The values of external diffusion coefficient, k_f, increase by the decreasing temperatures. The change in k_f depends on the surface area and pore distribution of AS. The AS has micropores and external diffusion is more difficult with the low temperatures.

The internal-pore diffusivities were determined using Equation (11). The adsorption data in Table 7 show that the internal-pore diffusion coefficients increase with the increasing temperatures.

Table 6. Kinetic parameters of adsorption.

Temperature	25°C	40°C	50°C
$q_{e.exp}$	54.011	55.015	55.721
Pseudo-first order			
q_e (mg/g)	54.888	54.288	35.989
k_1 (dk^{-1}) × 10^2	2.910	2.412	2.521
R^2	0.97	0.97	0.97
Pseudo-second order			
q_e (mg/g)	59.523	58.823	58.139
k_2 (g/mg.dk) × 10^4	1.311	1.850	2.590
h (mg/g.dk)	4.641	6.401	8.961
R^2	0.99	0.99	0.99
E_a (kJ/mol)	21.366		
Elovich			
β (g/mg)	0.089	0.093	0.098
a (mg/g dk)	12.822	17.779	25.484
R^2	0.97	0.97	0.98

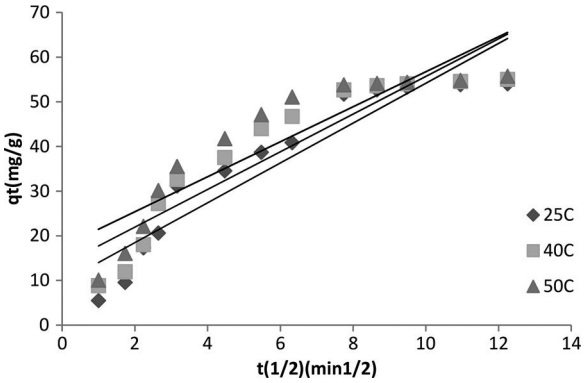

Figure 6. Intraparticle diffusion plots of MB adsorption.

Table 7. Diffusion parameters of adsorption.

Temperature (K)	298 K	313 K	323 K
Intraparticle diffusion			
k_1 (min^{-1})	4.459	4.216	3.918
C	9.545	13.513	17.547
R^2	0.87	0.85	0.84
External-film diffusion			
$K_f \times 10^7$ (m/min)	4.39	4.58	4.73
R^2	0.92	0.91	0.94
Internal-pore diffusion			
$D \times 10^{14}$ (m^2/min)	5.27	7,12	8.19
R^2	0.89	0.92	0.93

Table 8. Comparison of maximum adsorption capacity for the adsorption of MB by different adsorbents.

Adsorbent	q_m (mg/g)	Reference
Carbon nanotube	48.68	Lunhong et al. (2011)
Membrane	46.23	Auta and Hameed (2014)
Rice hull ash	17.10	Chen et al. (2012)
Coconut bunch waste	70.92	Hameed, Mahmoud, and Ahmad (2008)
Cocongrass	27.40	Su et al. (2014)
Apricot stone	4.11	Aygün, Yenisoy-Karakas, and Duman (2003)
Walnutt shell	3.52	Aygün, Yenisoy-Karakas, and Duman (2003)
Almond shell	66.67	Present study

As compared with the data reported in literature (Table 8), the AS have a relatively higher adsorption capacity than other natural biomasses reported in literature, indicating the potential of AS as a low-cost adsorbent for MB removal.

4. Conclusion

AS can be used as adsorbent for removal of MB from its aqueous solution.

The adsorption of MB onto AS showed an inclination to follow the Langmuir isotherm and Redlich–Peterson.

The kinetics of MB adsorption onto AS was examined using the pseudo-first-order, pseudo-second-order, and Elovich kinetics models. The adsorption kinetics followed the pseudo-second-order kinetic model.

The adsorption of MB onto AS was controlled by external diffusion. The rate of adsorption of MB was very high during the first 20 min. This was followed by a slower rate, and gradually approached a plateau.

References

Altenor, S., B. Carene, E. Emmanuel, J. Lambert, J. Ehrhardt, and S. Gaspard. 2009. Adsorption studies of methylene blue and phenol onto vetiver roots activated carbon prepared by chemical activation. *Journal of Hazardous Materials* 165:1029–39. doi:10.1016/j.jhazmat.2008.10.133.

Auta, M., and B. H. Hameed. 2014. Chitosane-clay composite as highly effective and lowcost adsorbent for batch and fixed-bed adsorption of methylene blue. *Chemical Engineering Journal* 237:352–61. doi:10.1016/j.cej.2013.09.066.

Aygün, A., S. Yenisoy-Karakas, and I. Duman. 2003. Production of granular activated carbon from fruit stones and nut shells and evaluation of their physical, chemical and adsorption properties. *Microporous and Mesoporous Materials* 66 (2–3):189–95. doi:10.1016/j.micromeso.2003.08.028.

Barrett, P. E. P., L. G. Joyner, and P. P. Halenda. 1951. The determination of pore volume and area distribution in porous substance. I. Computations from nitrogen isotherms. *Journal of the American Chemical Society* 73:373–80. doi:10.1021/ja01145a126.

Chen, S., J. Zhang, C. Zhang, Q. Yue, Y. Li, and C. Li. 2010. Equilibrium and kinetic studies of methyl orange and methyl violet adsorption on activated carbon derived from Phragmites austries. *Desalination* 252:149–56. doi:10.1016/j.desal.2009.10.010.

Chen, X., S. Lv, S. Liu, P. Zhang, A. Zhang, J. Sun, and Y. Ye. 2012. Adsorption of methylene blue by rice hull ash. *Separation Science and Technology* 47:147–56. doi:10.1080/01496395.2011.606865.

Dubinin, M. M., and L. V. Radushkevich. 1947. The equation of the characteristic curve of activated charcoal. *Proceedings of the Academy of Sciences, Physical Chemistry Section* 55:331–37.

Dutta, S., J. K. Basu, and R. N. Ghar. 2011. Studies on adsorption of p-nitrophenol on charred saw-dust. *Separation and Purification Technology* 21:227–35. doi:10.1016/s1383-5866(00)00205-7.

Freundlich, H. M. F. 1906. Uber dye adsorption in lusungen. *Physical Chemistry* 57:385–470.

Hameed, B. H., D. K. Mahmoud, and A. L. Ahmad. 2008. Equilibrium modeling and kinetic studies on the adsorption of basic dye by a low-cost adsorbent: Coconut (cocos nucifera) bunch waste. *Journal of Hazardous Materials* 158 (1):65–72. doi:10.1016/j.jhazmat.2008.01.034.

Haque, E., J. W. Jun, and S. H. Jhung. 2011. Adsorptive removal of methyl orange and methylene blue from aqueous solution with a metal-organic framework material, iron terephthalate (MOF-235). *Journal of Hazardous Materials* 185:507–11. doi:10.1016/j.jhazmat.2010.09.035.

Ho, Y. S., and G. Mckay. 1998. Sorption of dye from aqueous solution by peat. *Chemical Engineering Journal* 70:115–24. doi:10.1016/s0923-0467(98)00076-1.

Koble, R. A., and T. E. Corrigan. 1952. Adsorption isotherm for pure hydrocarbons. *Industrial and Engineering Chemistry* 44:383–87.

Kumar, K. V., K. Porkodi, and F. Rocha. 2008. Isotherms and thermodynamicsby linear and non-linear regression analysis for the sorption of methylene blue onto activated carbon: Comparison of various error functions. *Journal of Hazardous Materials* 151:794–804. doi:10.1016/j.jhazmat.2007.06.056.

Langmuir, I. 1918. The adsorption of gases on plane surfaces of glass, mica and platinum. *Journal of the American Chemical Society* 40:1361–68.

Lunhong, A., Z. Chunying, L. Fang, L. Ming, M. Lanying, and J. Jing. 2011. Removal of methylene blue from aqueous solution with magnetite loaded multi-wall carbon nanotube: Kinetic, isotherm and mechanism analysis. *Journal of Hazardous Materials* 198:282–90. doi:10.1016/j.jhazmat.2011.10.041.

Othman, Z. A. A., M. A. Habila, and A. Hashem. 2012. Removal of zinc (II) from aqueoussolutions using modified agricultural wastes: Kinetics and equilibrium studies. *Arabian Journal of Geosciences* 6:4245–55. doi:10.1007/s12517-012-0672-9.

Othman, Z. A. A., M. A. Habila, A. Rahmat, and M. S. E. Hassouna. 2013. Kinetic and thermodynamic studies for methylene blue adsorption using activated carbon prepared from agricultural and municipal solid wastes. *Asian Journal of Chemistry* 25:8301–06. doi:10.14233/ajchem.2013.14723.

Rafatullah, M., O. Sulaiman, R. Hashim, and A. Ahmad. 2010. Adsorption of methylene blue on low-cost adsorbents: A review. *Journal of Hazardous Materials* 177:70–80. doi:10.1016/j.jhazmat.2009.12.047.

Redlich, O., and D. I. Peterson. 1959. A useful adsorption isotherm. *The Journal of Physical Chemistry* 63:1024–26. doi:10.1021/j150576a611.

Ruthven, D. M. 1984. *Principles of adsorption and adsorption processes*. New York, NY: Wiley.

Sarıcı-Ozdemir, C. 2014. Removal of methylene blue by activated carbon prepared from waste in a fixed-bed column. *Particulate Science and Technology* 32:311–18. doi:10.1080/02726351.2013.851132.

Sips, R. 1948. Combined form of Langmuir and Freundlich equations. *The Journal of Chemical Physics* 16:490–95.

Srıvastova, S. K., R. Tyagı, and N. Pant. 1989. Adsorption of heavy metal ions on carbonaceous material developed from the waste slurry generated in local fertilizer plants. *Water Research* 23:1161–65. doi:10.1016/0043-1354(89)90160-7.

Streat, M., J. W. Patrıck, and M. J. Camporro Perez. 1995. Sorption of phenol and parachlorophenol from water using conventional and novel activated carbons. *Water Research* 29:467–72. doi:10.1016/0043-1354(94)00187-c.

Su, C. X. H., T. T. Teng, A. F. M. Alkarkhi, and L. W. Low. 2014. Imperata Cylindrica (Cogongrass) as an adsorbent for methylene blue dye removal: Process optimization. *Water, Air, & Soil Pollution* 225:1941–52. doi:10.1007/s11270-014-1941-x.

Temkin, M. J., and V. Pyzhev. 1940. Recent modifications to Langmuir isotherms. *Acta Physical Chemistry* 12:271–79.

Toth, J. 1971. State equations of the solid gas interface layer. *Acta Chimica (Academiae Scientiarum) Hungaricae* 69:311–17.

Weber, W. J., J. M. Asce, and J. C. Morrıs. 1973. Kinetics of adsorption on carbon from solution in: Proceedings of the American Society of Civil Engineers. *Journal of the Sanitary Engineering Division* 89:31–59.